A density-functional theory investigation on desorption of O_2 on Sn(111) and its comparison with initial oxidation on the X(111) (X=Si, Ge, Sn, Pb) surfaces*

Hu Zi-Yu(胡自玉), Wan Ping-Yu(万平玉), Hou Zhi-Ling(侯志灵), and Shao Xiao-Hong(邵晓红)†

College of Science, Beijing University of Chemical Technology, Beijing 100029, *China*

(Received 1 April 2012; revised manuscript received 10 June 2012)

The first-principles calculations are performed to investigate the adsorption of O_2 molecules on an Sn(111) 2×2 surface. The chemisorbed adsorption precursor states for O_2 are identified to be along the parallel and vertical channels, and the surface reconstructions of Sn(111) induced by oxygen adsorption are studied. Based on this, the adsorption behaviours of O_2 on X(111) (X=Si, Ge, Sn, Pb) surfaces are analysed, and the most stable adsorption channels of O_2 on X(111) (X=Si, Ge, Sn, Pb) are identified. The surface reconstructions and electron distributions along the most stable adsorption channels are discussed and compared. The results show that the O_2 adsorption ability declines gradually and the amount of charge transferred decreases with the enhancement of metallicity.

Keywords: O_2 adsorption, Sn(111) surface, precursor states, surface reconstructions

PACS: 68.43.Bc, 68.43.Fg, 81.65.Mq, 87.57.nf **DOI:** 10.1088/1674-1056/21/12/126803

1. Introduction

Tin oxides have received much attention, owing to their applications in high conductivity heat reflectors,[1,2] gas sensors,[3−5] and catalysts.[6−10] The first stage of catalysts and gas sensing actions are attributed to the preadsorption of oxygen onto the Sn surface.[11−14] The initial oxidation reaction kinetics can be significantly influenced by the precursor states. However, few studies have focused on the oxygen molecules adsorbed on a pure Sn surface. In addition, it is difficult to observe the molecule/Sn interaction at an atomic level in experiment, and the surface reconstruction phenomenon always occurs in the process of the initial adsorption, which is important for understanding the oxidation behaviours of chemisorptions and catalytic reactions on the atomic scale.[15,16] Therefore, a deeper understanding of adsorption behaviours at an atomistic and a quantum mechanical level is necessary. On the other hand, the elements of Si, Ge, Pb in the fourth main group have similar electronic structures, and Si, Ge and Sn exhibit the same lattice structures. Therefore, it is of interest to explore whether there are similar behaviours on the Si, Ge, Sn, and Pb surfaces.

Motivated by these questions, we systematically study the adsorption behaviours of the O_2 molecule on the Sn(111) surface and compare the oxidation on X(111) (X=Si, Ge, Pb) using the first-principles calculations. The results show that the adsorption of the O_2 molecule produces a molecular precursor, according well with previous studies.[17−24] More interestingly, it is found that the surfaces of X(111) (X=Si, Ge, Sn) induced by oxygen adsorption are reconstructed. The electron distributions and densities of states along the most stable adsorption channel on X(111) (X=Si, Ge, Sn, Pb) surfaces show that the interaction gradually declines with the enhancement of metallicity.

2. Computational method

The calculations are performed by using the spin-polarized version of the Vienna *ab initio* simulation package (VASP)[25] with the projector-augmented-wave (PAW)[26] pesudopotentials and plane waves. The wave functions are expanded in a plane-wave basis with an energy cutoff of 400 eV. The atomic positions

*Project supported by the National Natural Science Foundation of China (Grant No. 51102009) and the Fundamental Research Funds for the Central Universities, China (Grant No. JD1109).

†Corresponding author. E-mail: shaoxh@mail.buct.edu.cn

© 2012 Chinese Physical Society and IOP Publishing Ltd

are optimized by the conjugate gradient method[27] with an energy convergence of up to 0.1 meV. Periodic slabs consisting of six layers separated by a 20-Å (1 Å=0.1 nm) vacuum region are used, which is found to be sufficiently convergent. Oxygen molecules are placed on one side of the slab, namely on the top of the surface. An energy broadening[28] of 0.01 eV is chosen to smear the occupation of the bands around $E_{\rm F}$ by using a Fermi–Dirac distribution and extrapolating to $T = 0$ K. The Brillouin-zone summation is performed with a $7\times7\times1$ Monkhorst–Pack[29] k-point grid for all the $p(2 \times 2)$ surface cells calculated. The spin-polarization correction is included.

To test the accuracy of the plane-wave basis set and the pseudopotentials used, the lattice constants of X (X=Si, Ge, Sn, Pb) and the bond-length of isolated O_2 are fully optimized. The obtained lattice constants are 5.47, 5.76, 6.64, and 5.03 Å for Si, Ge, Sn, and Pb, which accord with the experimental[30] values of 5.43, 5.66, 6.49, and 4.95 Å, respectively. The calculated bond-length of an isolated O_2 molecule is 1.235 Å, which is in good agreement with the experimental value of 1.21 Å.[29]

The stability of an adsorption site is determined by an average adsorption energy of the adsorbed oxygen molecule, which is defined as (in units of eV per O atom)

$$E_{\rm ad} = -\frac{1}{2}[E_{\rm O_2+film} - E_{\rm film} - E_{\rm O_2}], \qquad (1)$$

where $E_{\rm O_2+film}$, $E_{\rm film}$, and $E_{\rm O_2}$ are the total energy of the slabs containing oxygen molecules, that of the corresponding clean $X(111)$ slab, and that of a free O_2 molecule, respectively. The stability of an adsorption site is also determined by the adsorption energy. Therefore, when one O_2 molecule stays at the site with the largest adsorption energy, the location is the most stable and energetically favourable site.

3. Precursor adsorption state of O_2 on the Sn(111) surface

We first study the molecular chemisorption of oxygen on the (2×2) structure of Sn(111). As a first stage of the formation of tin oxidation, a deeper understanding of the adsorption would provide a basis for more detailed characteristics of tin oxidation behaviours.

All the possible vertical and flat adsorption configurations of the molecule on the Sn surface are examined carefully. The O_2 molecule is centred over the top (T), hcp hollow (HH), fcc hollow (FH), and bridge (B) sites depicted in Fig. 1(a). At each high-symmetry site, the O_2 molecule possesses three different adsorbed orientations along the x (i.e., [011]), y (i.e., [211]), z (i.e., [111]) directions, respectively. Therefore, 12 high-symmetry adsorption channels for the O_2 molecule on the Sn surface are calculated in this work.

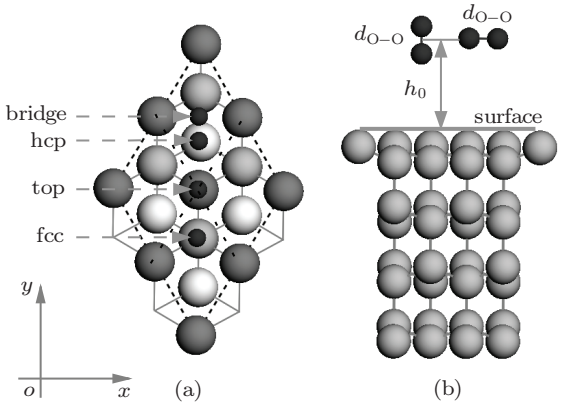


Fig. 1. (a) Four on-surface adsorption sites on the $p(2\times2)$ surface cell of $X(111)$ (X=Si, Ge, Sn, Pb). (b) The sketch map showing that the molecule (with vertical or parallel orientation) is initially away from the surface with a height of h_0.

In each case, the centre of the O_2 molecule is initially set to be 4 Å above the optimized Sn(111) surface shown in Fig. 1(b). After structural optimization, we obtain eight molecular adsorption states. These eight molecular adsorption states are represented for the O_2 orientation initially set to be along x and y directions. The final adsorption configurations are then examined. It is found that the final configurations in all cases are changed, and the oxygen molecules no longer stay at the initial high-symmetry (HS) site. To investigate the surface reconstruction distinctly, two kinds of adsorption forms are defined according to the coordinations on the surface: backbond oxidation, corresponding to the oxygen molecules parallel to the surface, and offsetbond oxidation, corresponding to the oxygen molecules rotating at an angle with respect to the surface. The final relaxed stable structures are shown in Fig. 2. It can be concluded that the linear oxygen molecule along HS-x channels (B-x, FH-x, HH-x, or T-x) for backbond oxidation (Fig. 2(A)–2(D)) is bonded with two tin surface atoms and the

molecular axis parallels to the surface. On the other hand, the linear oxygen molecule along the other HS-y channels (B-y, FH-y, HH-y, or T-y) for offset-bond oxidation are presented in Figs. 2(E)–2(H). As can be seen, the oxygen molecule is bonded with three top tin atoms (except for T-y) and offsets the surface tin atoms. Meanwhile, the deviation of the top surface tin atoms induced by the oxygen molecule is about 0.3 Å. Therefore, the surface reconstruction is apparent. The two oxygen atoms are drawn closer to the surface, and the distances between the oxygen atom (dark colour) and its bonded top-two surface tin atoms (white colour) are shown in Figs. 2(A)–2(H). The top views of these optimized most stable structures of (Figs. 2(A)–2(H) are shown in Figs. 2(a)–2(h). It can be seen that all the sites of oxygen molecules adsorbed on surfaces move from the initial sites. Especially, the initial bridge-site and top-site exhibit apparent deviations, so that it is difficult to distinguish the initial adsorption sites on the optimized stable structures.

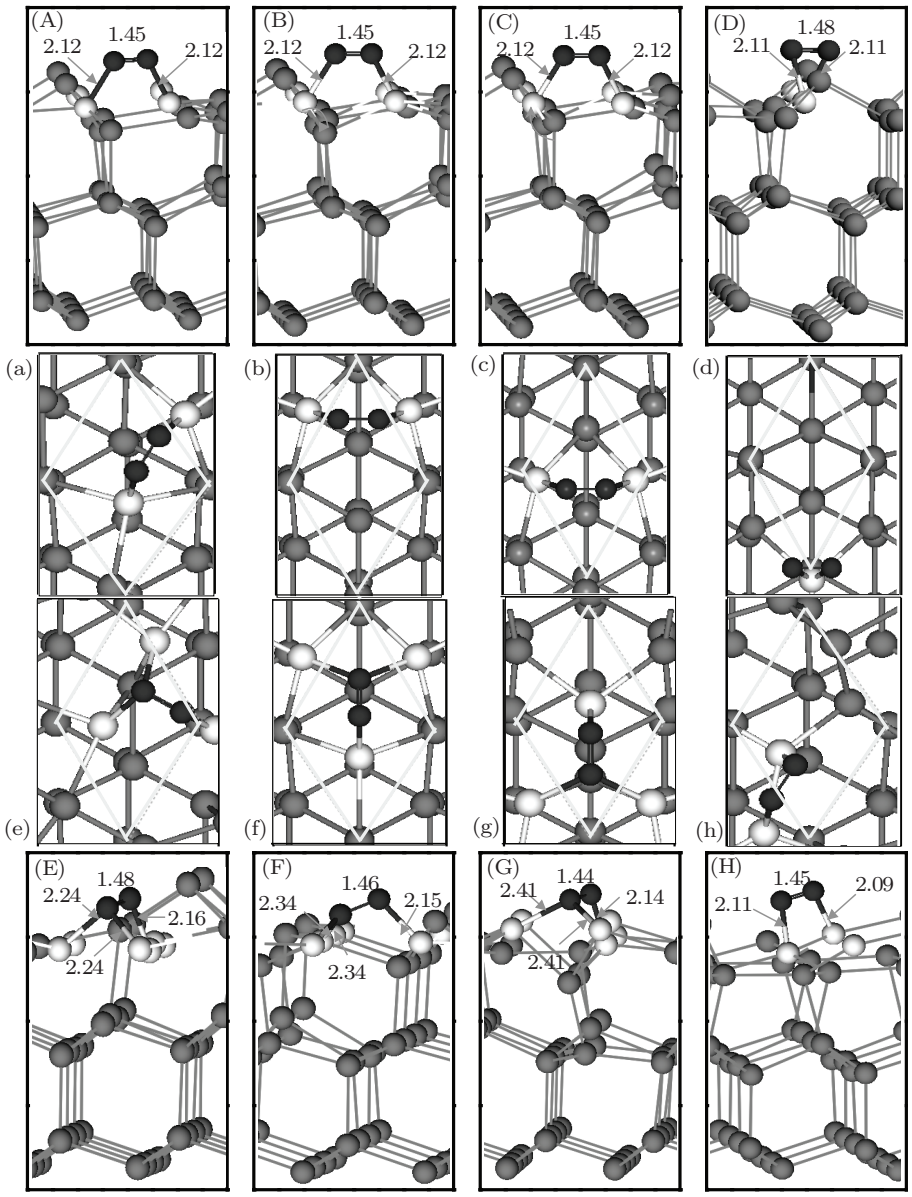


Fig. 2. Optimized structures for O_2 chemisorptions on the Sn(111)-(2×2) surface. The formation of backbond adsorption of the O_2 molecule is initially along the B-x, FH-x, HH-x, and T-x channels (A)–(D). The formation of offset-bond adsorption of the O_2 molecule is initially along the B-y, FH-y, HH-y, and T-y channels (E)–(H). Note that the two row panels (a)–(h) in the middle are the top views of the optimized structures for eight O_2 chemisorbed on the Sn(111) correspondingly. Oxygen atoms are represented in dark balls, tin in dark gray balls, and the surface Sn atoms connected with oxygen atoms in white balls as remarked. The bond-length of oxygen molecules and O–Sn are also listed in the panels.

The molecular adsorption energy (E_{ad}), O–O bond length (d), molecular magnetic moment (MM), and work function (Φ) are calculated. As shown in Table 1, the trending of the O–O bond length (d) can characterize the amplitude of the molecular adsorption energy (E_{ad}). It is thus found that the molecular MM and work function of the backbond oxidation forms are greater than those of the offset-bond oxidation forms. This phenomenon can be explained by the fact that the distance of the oxygen molecule to the surface Sn atoms of the offset-bond oxidation forms is much shorter than that of backbond oxidation forms, which makes orbital hybridization and charge transfer more intensive. Among all the relaxed configurations, the FH-y configuration is the most stable with the largest molecular adsorption energy (~ 0.915 eV per atom). In this channel, the height of the linear molecule decreases, the molecular MM nearly disappears, and the molecular bond length is as large as 1.461 Å, indicating that the interaction between O_2 and the Sn(111) surface is so prominent.

Table 1. The calculated values of adsorption energy per atom (E_{ad}), O–O bond length (d), molecular magnetic moment (MM), and work function (Φ) for chemisorptions along different channels.

Channel	E_{ad}/meV	d/Å	MM/μ_B	Φ/eV
T-x	780	1.48	0.73	4.71
T-y	754	1.45	0.09	4.67
B-x	777	1.45	1.23	4.65
B-y	823	1.48	0.00	4.49
HH−x	774	1.45	1.24	4.64
HH-y	631	1.44	0.00	4.54
FH-x	776	1.45	1.19	4.65
FH-y	915	1.46	0.00	4.49

In order to obtain further insight into the characteristics of the chemisorbed molecular state in the O_2/Sn(111) system and explain how the O_2 molecule interacts with Sn(111) surface, the orbital-resolved site-projected densities of states (PDOSs) for the O_2 molecules in the most stable FH-y entrance and the topmost Sn layer are plotted in Figs. 3(a) and 3(b), respectively. By comparing with the case of a free O_2 molecule, one can see that both σ and π molecular orbitals (MOs) of the chemisorbed O_2 in the FH-y entrance undergo the fundamental changes. Firstly, the spin splitting of both bonding and anti-bonding MOs vanishes. Secondly, the prominent changes of the spin-split PDOS peaks for the two lowest-energy bonding and antibonding σ MOs of the free O_2 molecule indicate its strong perturbation by interacting with the Sn(111) surface. Thirdly, the PDOS peaks for the two nearly degenerate bonding σ_p and π_p MOs around $E = -6.0$ eV are broadened largely after the chemisorptions states have been merged together, which leads to the amplitude becoming much weaker than that for a free O_2. Finally, near the Fermi level, the PDOS peaks for the two nearly degenerate antibonding π_p^* MOs are also broadened. The transfer of electrons from the adsorbed molecule into the unoccupied metal surface and a back donation of electrons from the occupied metal states into the antibonding MOs are not pronounced. Maybe this exchange is achieved only through the interaction between the p orbitals of the Sn(111) surface and the adsorbed molecule.

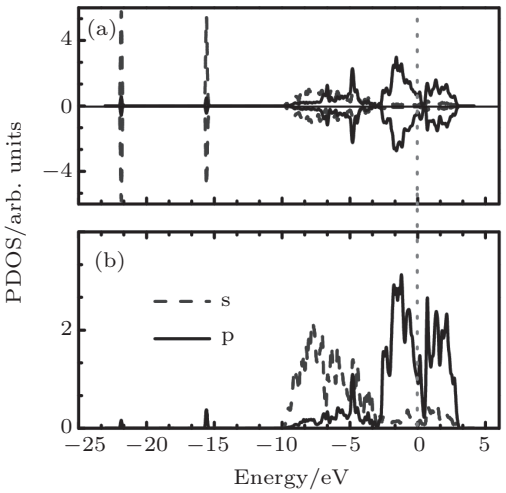


Fig. 3. Orbital-resolved PDOSs for the chemisorbed O_2 molecule (a) and the topmost Sn layer (b) along the FH-y channel. The Fermi energy is set at zero. Note that the O_2 is plotted in a spin-split form.

4. Adsorption of O_2 on $X(111)$ (X=Si, Ge, Sn, Pb) surfaces

To investigate the adsorption mechanism of the initial oxidation procedure, the adsorption behaviours of O_2 molecules on $X(111)$ (X=Si, Ge, Sn, Pb) surfaces are systemically analysed. Twelve initial geometries for each $X(111)$ slab are constructed, and the extensive optimizations are performed. Note that on one side of the slabs of Si and Ge, the bottom atomic layers are saturated by hydrogen in order to maintain the same population ratio of the $p(2 \times 2)$ surface.[32] The most stable structures with the largest adsorption energies of the four systems are shown in Fig. 4. Figure 4(a) presents the most stable structure of O_2/Si(111). It is demonstrated that the O_2

molecule can dissociate without overcoming any barrier on the clean Si(111) surface, which results in an ad-ins structure, where "ad" denotes an O atom adsorbed on the top of the Si adatom, and "ins" means that an O atom is singly inserted into two Si adatom backbonds. The Si–O_{ad} bond length is 1.56 Å, which is similar to the bond length 1.54 Å of a free SiO molecule. The Si–O_{ins}–Si bond angle is somewhat smaller than that of the crystalline SiO_2 ($\sim$ e.g., 144° for α-quartz). The O_2 vibration frequency value and the PDOS calculated here show that the binding energy of the O 2p orbital (i.e., O_{ad} and O_{ins} atoms) is in good agreement with the experimental electron energy loss spectroscopy (EELS)[33–35] and ultraviolet photoelectron spectroscopy (UPS)[36–38] results, respectively. Figure 4(b) gives the most stable structure of O_2/Ge(111). The linear molecule is tilted with respect to the parallel surface and bonded to three top surface Ge atoms. The two oxygen atoms are drawn closer to the surface with distances of 1.94 Å, 2.22 Å, and 2.22 Å away from the Ge atoms. Our results suggest that one oxygen atom is doubly bonded to Ge atoms and the other oxygen atom is only tiltedly bonded with a Ge atom. This is different from the previous study of the O_2/Ge (100)[39] system, in which a more favourable energetic oxidation model suggests that each oxygen atom is bonded with a Ge atom. The most stable structure of O_2/Sn(111) is also shown in Fig. 4(c) for comparison. The 6-monolayer (ML) Pb film along the HH-x channel which has the largest adsorption energy is given in Fig. 4(d) as a representative to examine the structural and electronic properties of the O_2-adsorbed film. The bond length and the height of the oxygen molecule are listed in Fig. 4, which coincide well with the results of our previous study on the dissociation and adsorption of O_2/Pb(111),[20] and the centre of a parallel linear molecule exhibits a certain offset against the centre of the HH site after adsorption. In addition, the most stable channel of O_2/X(111) (X=Si, Ge, Sn) is along the same FH-y channel shown in Figs. 4(a)–4(c). Moreover, the reconstruction of the surface, induced by adsorption is examined. The deviation of the top surface atoms, influenced by an oxygen molecule is about 0.3 Å, and the distances of one oxygen molecule to surface atoms (white colour marked) are shown in the panels. However, there is a slight exception to Pb, which could be explained by the fact that the lattice structure of Pb is somewhat different from the others.

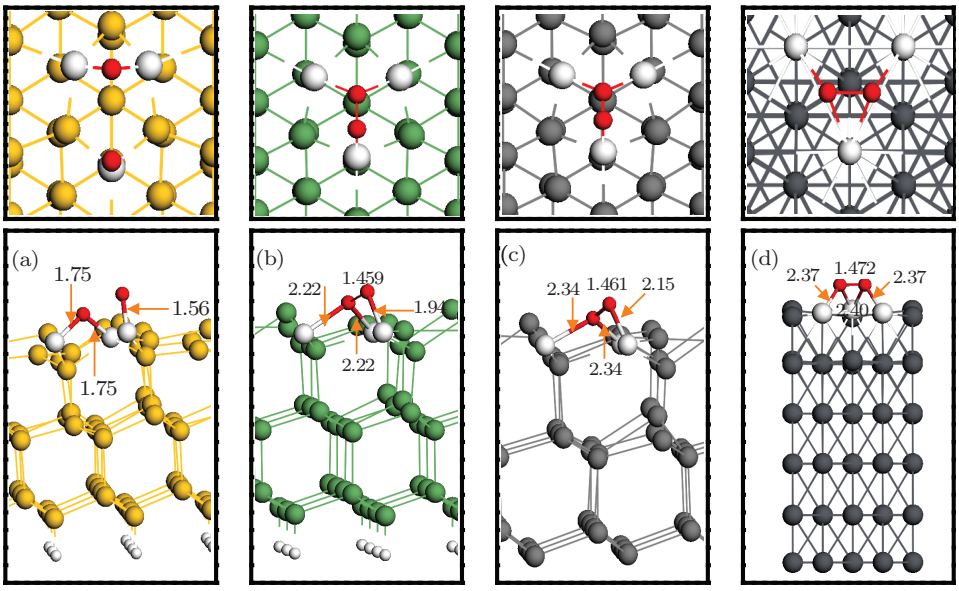


Fig. 4. (colour online) Optimized structures of the O_2 molecule along the most stable channel on the 6-ML Si(111), Ge(111), Sn(111), and Pb(111) films are presented in panels (a)–(d) for a comparison. The balls are represented in their elemental colours. Note that the surface atoms bonded with oxygen atoms are colored white. The distances of O–O and O–Sn are listed on the panels.

To further analyse the structures of these most stable adsorbed channels, the calculated values of molecular adsorption energy (E_{ad}), O–O bond length (d), work function (Φ), and the amount of charge transfer are listed in Table 2. As can be seen, the adsorption energy of the O_2 molecule weakens gradually, while the amount of charge transfer decreases. The results lead to a gradual increase of the oxygen molec-

ular bond, which indicates that some regular catalytic performances occur in the oxidation process of the four elements in the same group.

Table 2. Calculated values of oxygen molecular adsorption energy per atom (E_{ad}), O–O bond length (d), and work function (Φ), and the amount of charge transformation from the substrate to the chemisorbed O_2 molecule along the most stable channels of Si, Ge, Sn, and Pb surface.

Surface	E_{ad}/eV	d/Å	Φ/eV	(e)
Si(111)	2.88	–	5.48	1.60
Ge(111)	1.38	1.459	5.00	1.21
Sn(111)	0.92	1.461	4.49	1.09
Pb(111)	0.47	1.472	4.51	0.95

The values of the charge density difference ($\Delta\rho(r)$) of the O_2 molecule and 6-ML $X(111)$ (X=Si, Ge, Sn, Pb) films for the most stable chemical adsorption state were calculated (see Fig. 5), which are obtained by subtracting the electron densities of non-interacting component systems, $\rho_{X(111)}(r) + \rho_{O_2}(r)$ from the densities of $\rho_{O_2+X(111)}$ of the four systems subtracts, with the atomic positions of the component systems kept unchanged. A positive $\Delta\rho(r)$obviously represents charge accumulation, whereas a negative $\Delta\rho(r)$ represents charge depletion. Figures 5(a)–5(d) show clearly the charge transfers from X (X=Si, Ge, Sn, Pb) to O_2, which is consistent with the electronegativity difference between O and X atoms. The contour plots for the two-dimensional $\Delta\rho(r)$ in the plane containing two O atoms and parallel to the $X(111)$ surface, are correspondingly shown on the tops of three-dimensional charge transfer panels. The blue colour represents charge accumulation, and red (yellow) colour represents charge depletion. It can be easily seen that the charge moves from the substrate to the O_2 $\pi^*_\perp$ or $\pi^*_{||}$ antibonding states. The values of $\pi^*_\perp$ and $\pi^*_{||}$ indicate orientations of O_2 antibonding states perpendicular or parallel to the surface. Because of the charge transfer, the O–O bond length is extruded. The presence of an adatom and rest atom pair would be favourable for the initial O_2 adsorption on the Si(111) surface.[32] Figure 5(a) shows electron distributions in the occupied and unoccupied MOs in the vertical plane that contains both the Si adatom and rest atom. As shown in the figure, most of the electron density in the highest occupied molecular orbital (HOMO) resides around the rest atom. Only small electron densities in the HOMO and the lowest unoccupied molecular orbital (LUMO) are localized on the adatom site. These electron distributions can be used to explain the basic scanning tunneling microscope (STM) results that show Si adatoms are imaged brightly in both conditions of the filled state and empty state sample biases. From the contour plots of the charge density difference in Figs. 5(b)–5(d), one can see that there is an electron depletion area in the middle of the two oxygen atoms, indicating the O_2-to-surface π donation, and two electron accumulation areas around the two oxygen atoms representing the surface-to-O_2 π^* back donation.

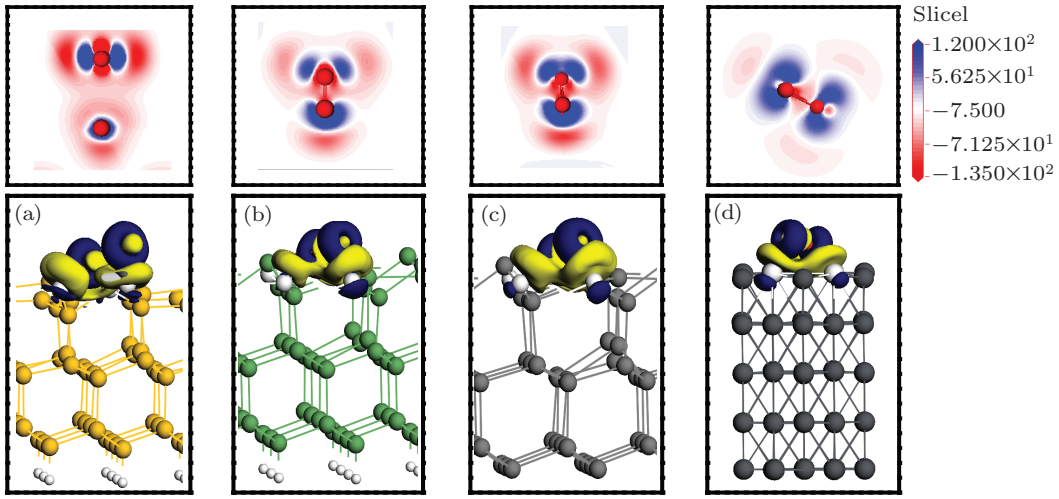


Fig. 5. (colour online) Three-dimensional charge transfers from X (X=Si, Ge, Sn, Pb) to O_2, with the isosurface value being ±0.03 Å. The contour plots for two-dimensional $\Delta\rho(r)$ in the plane containing the two O atoms and parallel to the $X(111)$ surface are correspondingly shown on the tops of three-dimensional charge transfer panels. The red (yellow) and blue areas indicate the charge depletion and accumulation around the O_2 molecule.

5. Conclusion

In this work, we systematically investigated the behaviours of O_2 molecules on Sn(111) surface using the spin-polarized first-principles calculations. The oxidation mechanism of the Sn(111) surface was analysed and the surface reconstruction was explicitly discussed. Two kinds of adsorption forms were found: backbond oxidation and offset-bond oxidation. Furthermore, the adsorption behaviours of O_2 molecules on $X(111)$ (X=Si, Ge, Pb) films were discussed. The comparisons of the adsorption behaviours, molecular magnetic moment, and work function among the O_2 molecules on $X(111)$ (X=Si, Ge, Sn, Pb) show that the O_2 adsorption ability declines gradually and the amount of charge transfer decreases with the enhancement of metallicity. Our study further provides a detailed physical picture for the adsorption of the O_2 molecule on $X(111)$ (X=Si, Ge, Sn, Pb) surfaces.

References

[1] Yamazoe N 1991 *Sens. Actuators* B **5** 7

[2] Gardner J W and Bartlett P N 1994 *Sens. Actuators* B **18** 211

[3] Seiyama T, Kato A, Fujiishi K and Nagatani M 1962 *Anal. Chem.* **34** 1502

[4] Ihogura K and Watson J 1993 *Stannic Oxide Gas Sensors* (Tokyo: CRC Press)

[5] Batzill M 2006 *Sensors-Basel* **6** 1345

[6] Nagasawa Y, Choso T, Karasuda T, Shimomura S, Ouyang F, Tabata K and Yamaguchi Y 1999 *Surf. Sci.* **226** 433

[7] Yamaguchi Y, Nagasawa Y, Murakami A and Tabata K 1998 *Int. J. Quantum Chem.* **69** 669

[8] Yamaguchi Y, Nagasawa Y, Shimomura S and Tabata K 1999 *Int. J. Quantum Chem.* **74** 423

[9] Henrich V E and Cox P A 1994 *The Surface Science of Metal Oxides* (Cambridge: Cambridge University Press) p. 247

[10] Batzill M and Diebold U 2005 *Prog. Surf. Sci.* **79** 47

[11] Boggs W E, Kachik R H and Pellissier G E 1961 *J. Electrochem. Soc.* **108** 1

[12] Powell R A and Spicer W E 1976 *Surf. Sci.* **55** 681

[13] Powell R A 1979 *Appl. Surf. Sci.* **3** 379

[14] Stander C M 1983 *Appl. Surf. Sci.* **16** 463

[15] Kung H H 1989 *Transition Metal Oxides, Surface Chemistry and Catalysis* (Amsterdam: Elsevier) pp. 259–273

[16] Somorjai G A 1994 *Annual Review of Physical Chemistry* **45** 721–751

[17] Schell-Sorokin A J and Demuth J E 1985 *Surf. Sci.* **157** 273

[18] Silvestre C and Shayegan M 1998 *Phys. Rev.* B **37** 10432

[19] Surnev L and Tikhov M 1982 *Surf. Sci.* **123** 505

[20] Yang Y, Zhou G, Wu J, Duan W H, Xue Q K, Gu B L, Jiang P, Ma X C and Zhang S B 2008 *J. Chem. Phys.* **128** 164705

[21] Ma H F, Xu M C, Yang B, Shi D X, Guo H M, Pang S J and Gao H J 2007 *Chin. Phys.* **16** 2661

[22] Lu H, Wang X D, Motai K, Hashizume T and Sakurai T 1992 *Acta Phys. Sin.* (Overseas Edition) **1** 191

[23] Yang Y 2010 *Chin. Phys.* B **19** 108201

[24] Hu Z Y, Yang Y, Sun B, Zhang P, Wang W C and Shao X H 2012 *Chin. Phys.* B **21** 016801

[25] Kresse G and Furthmuller J 1996 *Phys. Rev.* B **54** 11169 and references therein

[26] Kresse G and Joubert D 1999 *Phys. Rev.* B **59** 1758

[27] Teter M P, Payne M C and Allan D C 1989 *Phys. Rev.* B **40** 12255

[28] Weinert M and Davenport J W 1992 *Phys. Rev.* B **45** 13709

[29] Monkhorst H J and Pack J D 1976 *Phys. Rev.* B **13** 5188

[30] Kittel C 1976 *Introduction to Solid State Physics* (New York: Wiley) p. 368

[31] Huber K P and Herzberg G 1979 *Constants of Diatomic Molecules* (New York: Van Nostrand) p. 494

[32] Hoshino T and Nishioka Y 2007 *Phys. Rev.* B **61** 7

[33] Ibach H, Bruchmann H D and Wagner H 1982 *Appl. Phys.* A: *Solids Surf.* **29** 113

[34] Ibach H, Horn K, Dorn R and LÄuth H 1973 *Surf. Sci.* **38** 433

[35] HÄofer U, Morgen P, Wurth W and Umbach E 1985 *Phys. Rev. Lett.* **55** 2979

[36] Bozso F and Avouris Ph 1991 *Phys. Rev.* B **44** 9129

[37] Comtet G, Dujardin G, Hellner L, Hirayama T, Rose M, Philippe L and Besnard-Ramage M J 1995 *Surf. Sci.* **331** 370

[38] Sakamoto K, Doi S, Ushimi Y, Ohno K, Yeom H W, Ohta T, Suto S and Uchida W 1999 *Phys. Rev.* B **60** R8465

[39] Fan X L, Lau W M and Liu Z F 2009 *J. Phys. Chem.* C **113** 8786